Results

A. Optical microscopy (OM) observations:

Figures 3(a) through (d) are four optical micrographs of the alloys after being solution heat-treated at 900℃ for 1 hour and then quenched into ice brine rapidly. It is clearly seen that the as-quenched microstructure of alloy A ($Cu_{2.9}Mn_{0.1}Al$) was a plate-like martensite within the matrix, and that of alloy B ($Cu_{2.8}Mn_{0.2}Al$), C ($Cu_{2.7}Mn_{0.3}Al$) and D ($Cu_{2.6}Mn_{0.4}Al$) was a single phase. Based on the above results, it can be observed that the martensite start temperature would decrease with increasing manganese content. This result is in agreement with other researchers in Cu-Mn-Al alloy systems [28, 30-31].

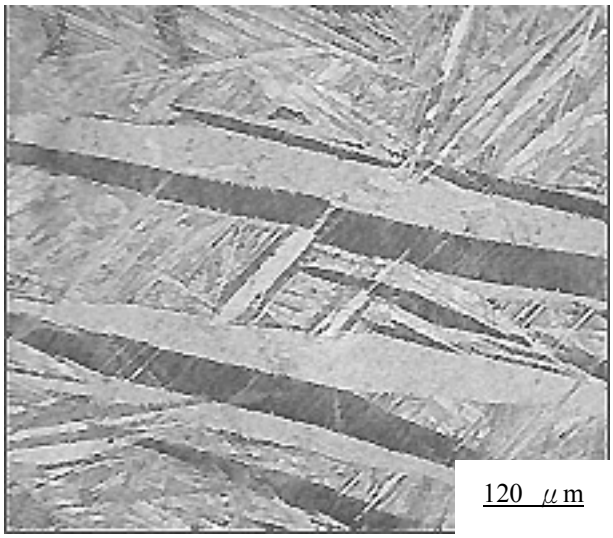

Fig. 3(a)

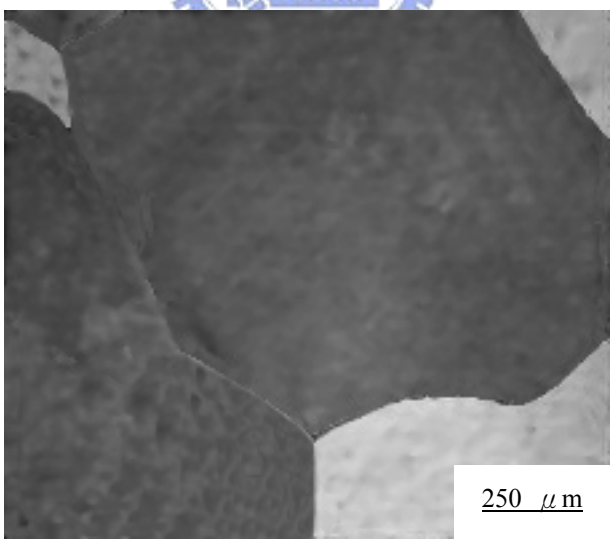

Fig. 3(b)

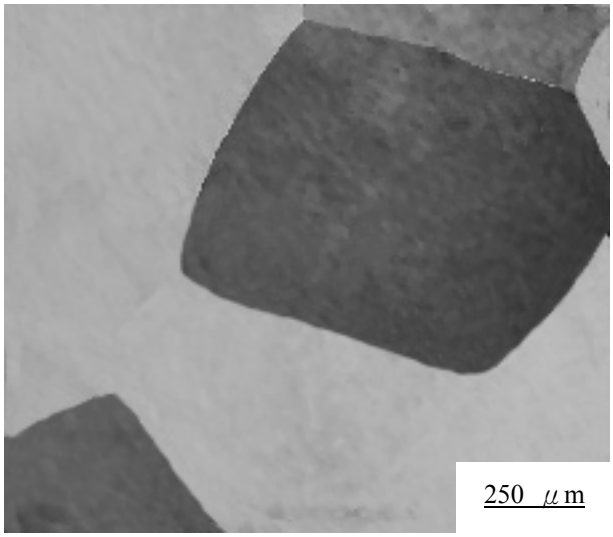

Fig. 3(c)

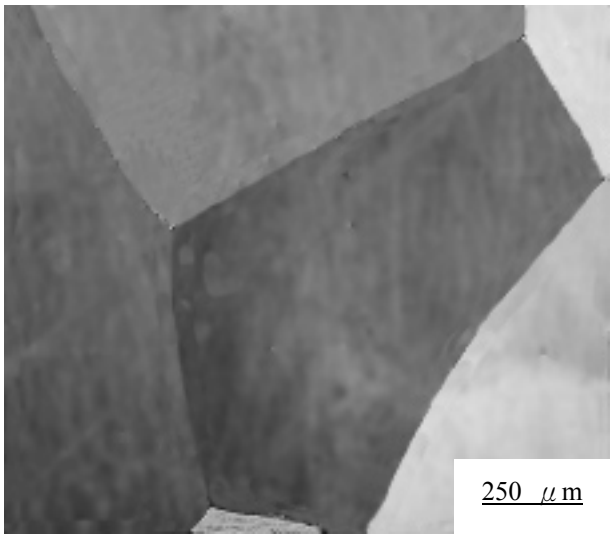

Fig. 3(d)

Fig. 3 Optical micrographs of the as-quenched alloys. (a) through (d) are alloy A ($Cu_{2.9}Mn_{0.1}Al$), B ($Cu_{2.8}Mn_{0.2}Al$), C ($Cu_{2.7}Mn_{0.3}Al$) and alloy D ($Cu_{2.6}Mn_{0.4}Al$), respectively.

B. Transmission electron microscopy (TEM) observation:

(a) Microstructure of $Cu_{2.9}Mn_{0.1}Al$ alloy

Figure 4(a) is a bright-field (BF) electron micrograph of the as-quenched $Cu_{2.9}Mn_{0.1}Al$ alloy (alloy A), clearly exhibiting a second phase with a plate-like morphology within the matrix. Figures 4(b) and (c) show two different selected-area diffraction patterns (SADPs) taken from a plate-like phase and its surrounding matrix. In these SADPs, it is seen that beside those reflection spots corresponding to the $D0_3$ phase [1, 28], extra spots caused the second phase are clearly visible. Compared with the previous studies in Cu-Al and Cu-Al-Ni alloys [28-31], it can be realized that the positions and streaking behaviors of the extra spots are the same as those of the γ_1' martensite with internal twins [28, 30-31]. The γ_1' martensite has an orthorhombic structure with lattice parameters a=0.440 nm, b=0.534 nm and c=0.422 nm [30, 32]. Figure 4(d) is a $(1\bar{2}1)$ γ_1' dark-field

(DF) electron micrograph, clearly revealing the presence of the plate-like γ_1' martensite. Accordingly, it is concluded that the as-quenched microstructure of the alloy A was $D0_3$ phase containing plate-like γ_1' martensite. This finding is similar to that reported by other workers in the Cu_3Al alloy [1, 27].

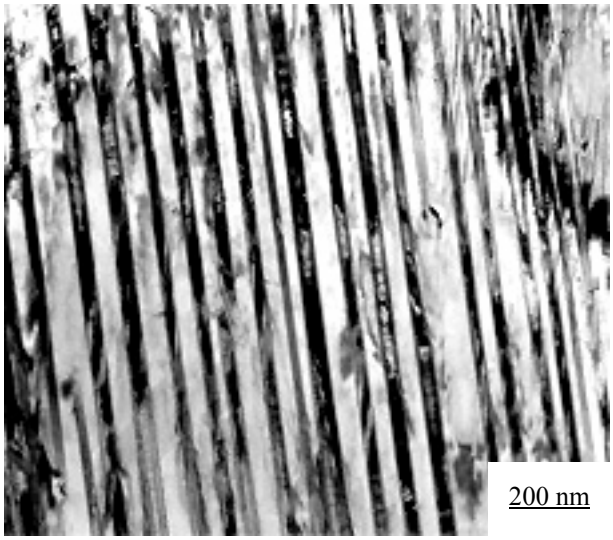
200 nm

Fig. 4(a)

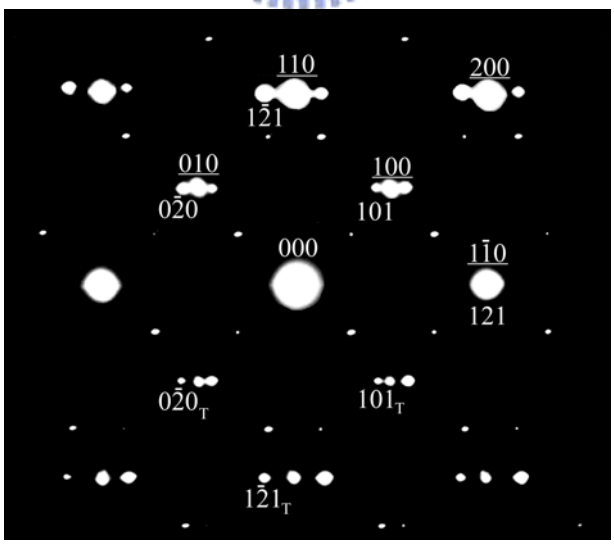
110
200
1$\bar{2}$1
010
100
0$\bar{2}$0
101
000
1$\bar{1}$0
121
0$\bar{2}$0$_T$
101$_T$
1$\bar{2}$1$_T$

Fig. 4(b)

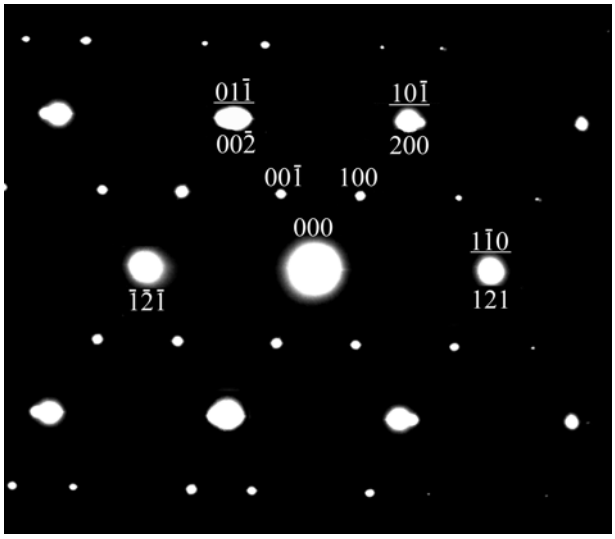

Fig. 4(c)

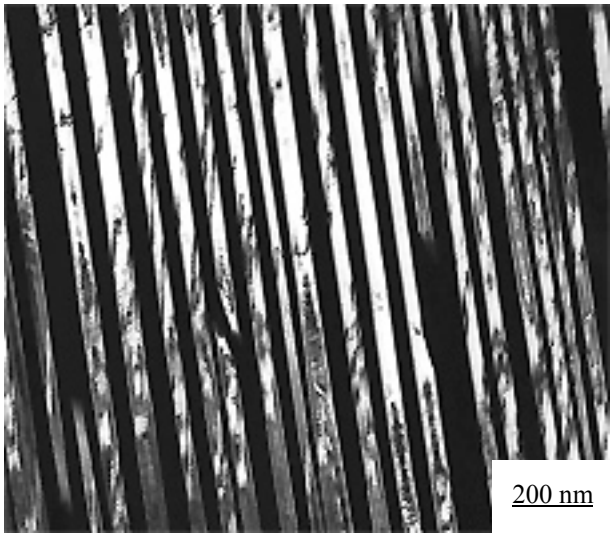

Fig. 4(d)

Fig. 4 Electron micrographs of the as-quenched alloy A. (a) BF, (b) and (c) two SADPs. The zone axes of the $D0_3$ phase , γ_1' martensite and internal twin are (b) [001], [$10\bar{1}$] and [$\bar{1}01$], (c) [111], [$2\bar{1}0$] and [$\bar{2}10$], respectively (<u>hkl</u>= $D0_3$ phase, hkl= γ_1' martensite, hkl_T=internal twin), (d) ($1\bar{2}1$) γ_1' martensite DF.

(b) Microstructure of $Cu_{2.8}Mn_{0.2}Al$ alloy

When the manganese content was increased to 5 at.% (X=0.2), no evidence of the γ_1' martensite could be detected. There were a high density of extremely fine precipitates with a mottled structure could be observed within the $D0_3$ matrix. A typical example is shown in Figure 5. Figure 5(a) is a BF electron micrograph of the $Cu_{2.8}Mn_{0.2}Al$ alloy (alloy B) in the as-quenched condition. Figures 5(b) and (c) show two different SADPs of the as-quenched alloy B. When compared with our previous studies in the $Cu_{2.2}Mn_{0.8}Al$ and Cu-14.6Al-4.3Ni alloys [25, 29], it is found, in these SADPs, that the extra spots with streaks could be derived from the L-J phase with two variants. Figure 5(d) is a (002) $D0_3$ DF electron micrograph of the same area as Figure 5(a), revealing the presence of the small B2 domains with a/4<111> anti-phase boundaries (APBs). Figure 5(e), a $(\bar{1}11)$ $D0_3$ DF electron micrograph, shows the presence of the fine

$D0_3$ domains with a/2<100> APBs. In Figures 5(d) and (e), it is seen that the sizes of both B2 and $D0_3$ domains are very small. Therefore, it is deduced that the $D0_3$ phase present in the as-quenched alloy was formed by an A2→B2→$D0_3$ continuous ordering transition during quenching [34-37]. Figure 5(f) is a ($0\bar{2}0$) L-J DF electron micrograph, exhibiting the presence of the extremely fine L-J precipitates. Based on the above observations, it was concluded that the as-quenched microstructure of the present alloy B was $D0_3$ phase containing extremely fine L-J precipitates, where the $D0_3$ phase was formed by the A2→B2→$D0_3$ continuous ordering transition during quenching.

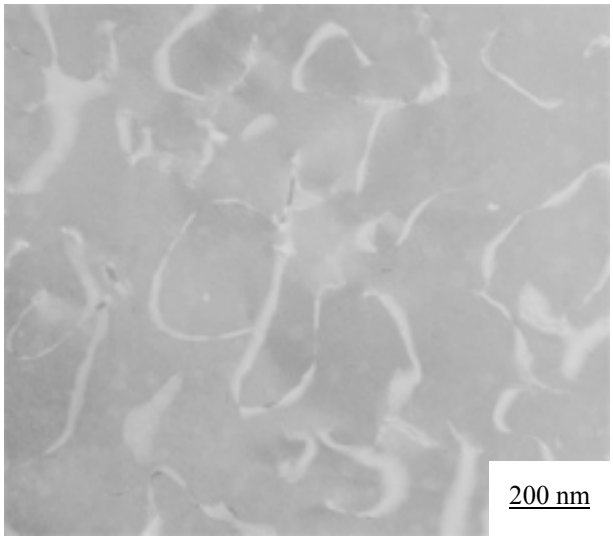

Fig. 5(a)

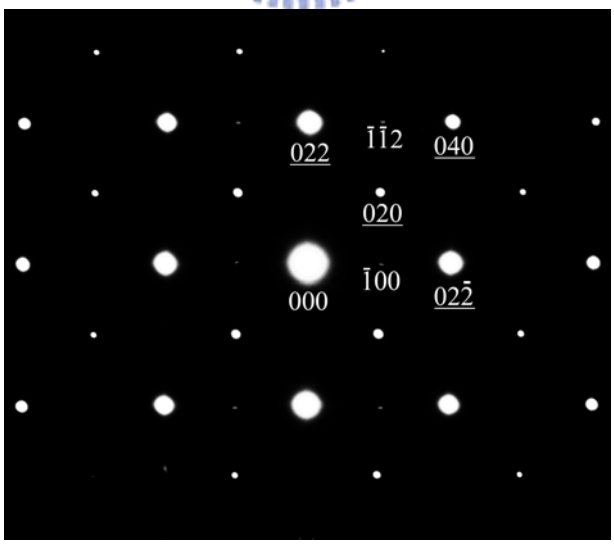

Fig. 5(b)

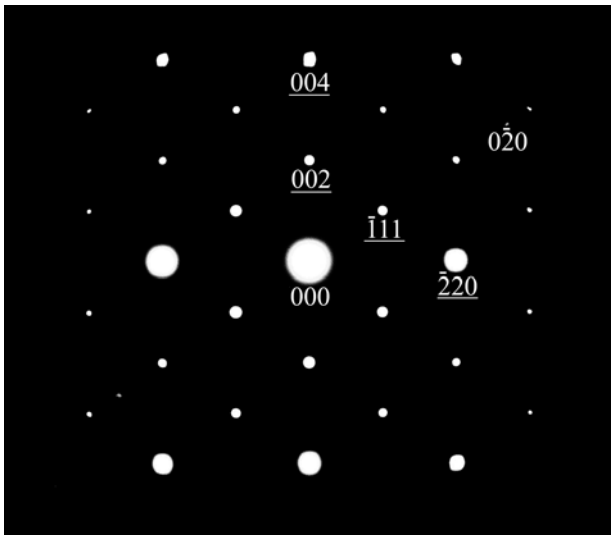

Fig. 5(c)

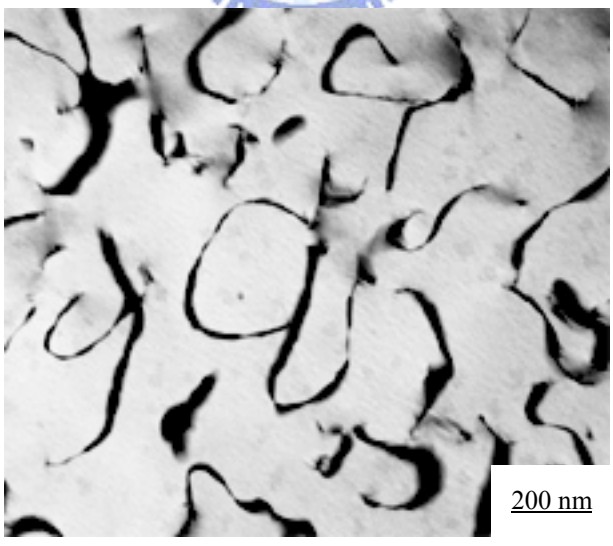

Fig. 5(d)

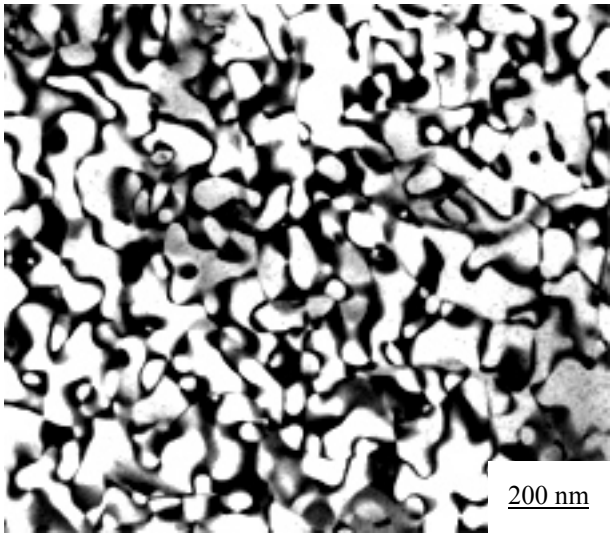

Fig. 5(e)

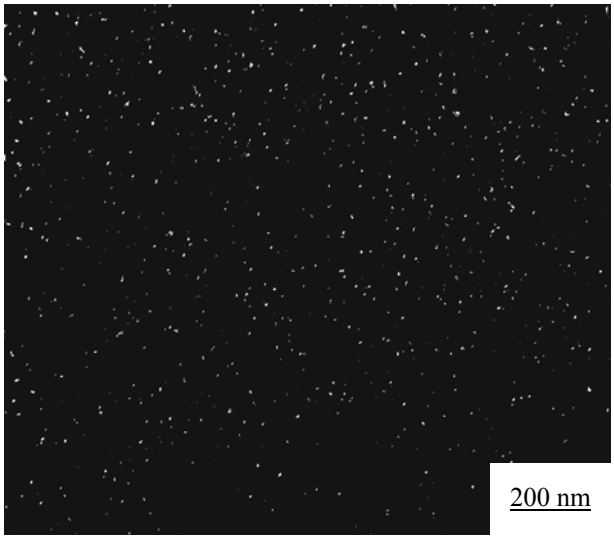

Fig. 5(f)

Fig. 5 Electron micrographs of the as-quenched alloy B. (a) BF, (b) and (c) two SADPs. The zone axes of the $D0_3$ phase are (b) [001] and (c) [110], respectively (<u>hkl</u>= $D0_3$ phase, hkl= L-J phase,), (d) and (e) (002) and ($\bar{1}11$) $D0_3$ DF, respectively, (f) ($0\bar{2}0$) L-J DF.

(c) Microstructure of $Cu_{2.7}Mn_{0.3}Al$ alloy

Transmission electron microscopy examinations of thin foils indicated that the as-quenched microstructure of the alloy C was also $D0_3$ phase containing extremely fine L-J precipitates, which is similar to that observed in the alloy B. An example is shown in Figure 6. Figures 6(a) is a BF electron micrograph of the $Cu_{2.7}Mn_{0.3}Al$ alloy (alloy C). Figure 6(b) and (c) are two different SADPs of the as-quenched alloy C. Figures 6(d) through (f) are (002) as well as $(\bar{1}11)$ $D0_3$ and $(0\bar{2}0)$ L-J DF electron micrographs of the alloy C in the as-quenched condition, respectively. By comparing Figures 5 and 6, it is clear that a slight increase of the manganese content would significantly raise the amount of the L-J precipitates; it would also increase the sizes of both B2 and $D0_3$ domains.

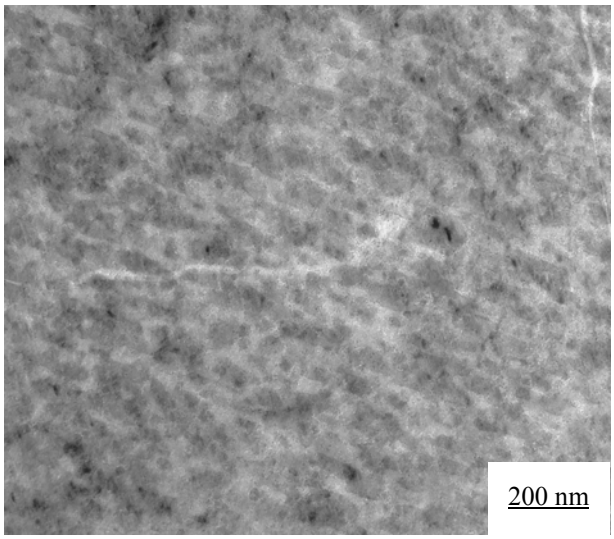

Fig. 6(a)

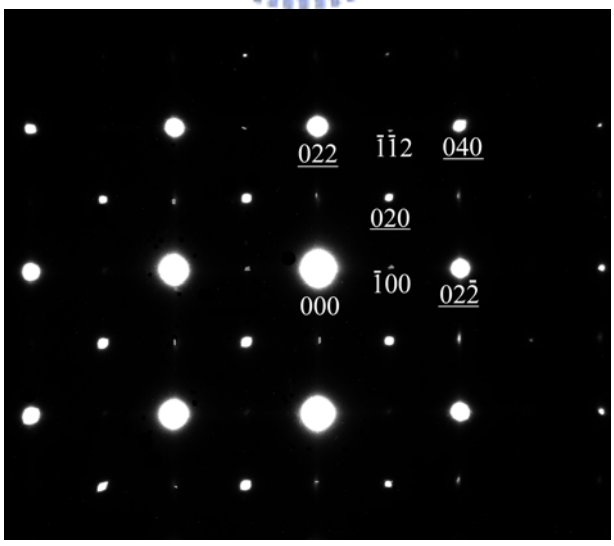

Fig. 6(b)

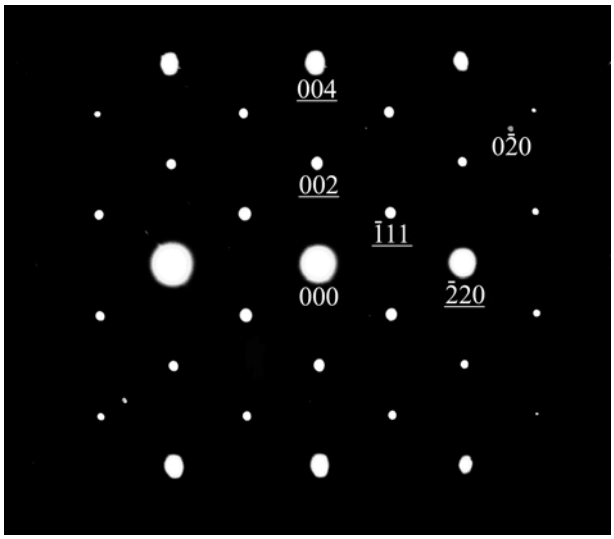

Fig. 6(c)

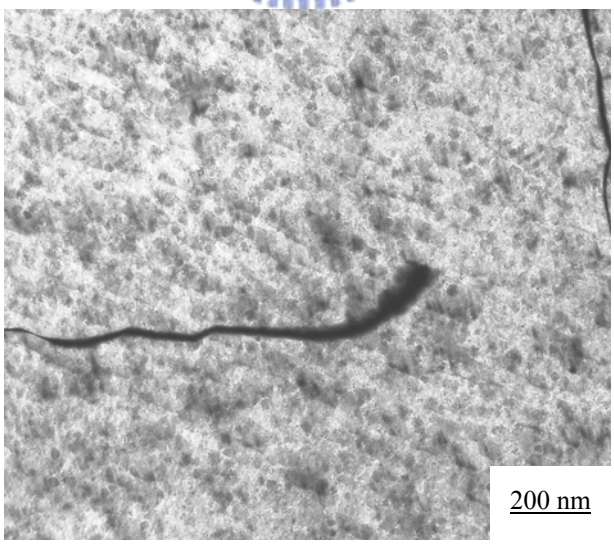

Fig. 6(d)

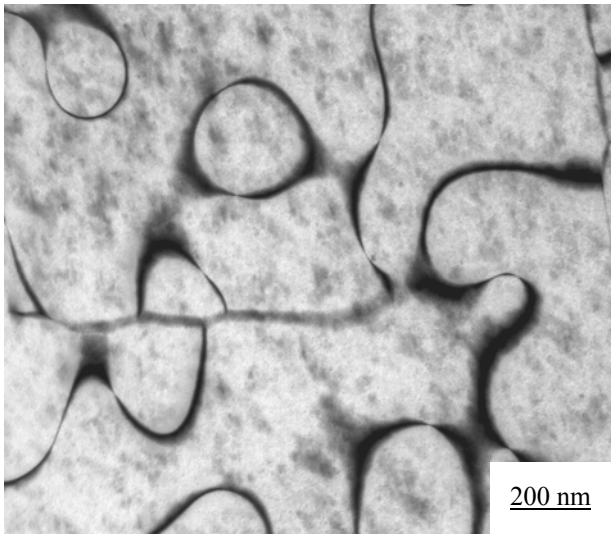

Fig. 6(e)

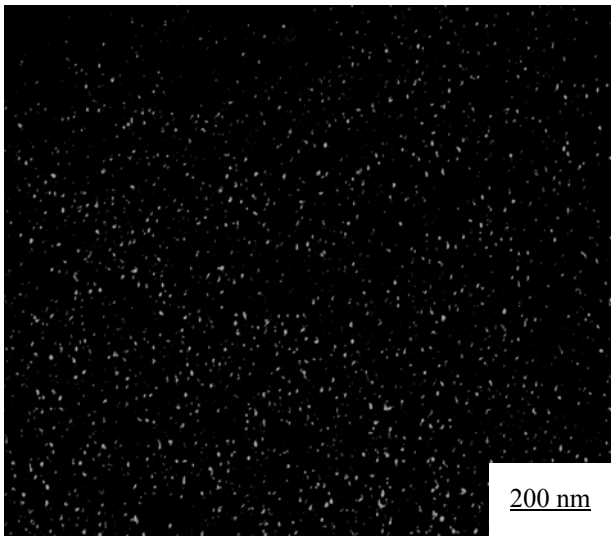

Fig. 6(f)

Fig. 6 Electron micrographs of the as-quenched alloy C. (a) BF, (b) and (c) two SADPs. The zone axes of the $D0_3$ phase are (b) [001] and (c) [110], (d) and (e) (002) and $(\bar{1}11)$ $D0_3$ DF, respectively, (f) $(0\bar{2}0)$ L-J DF.

(d) Microstructure of $Cu_{2.6}Mn_{0.4}Al$ alloy

Figure 7(a) is a BF electron micrograph of the as-quenched $Cu_{2.6}Mn_{0.4}Al$ alloy (alloy D), exhibiting a modulated structure within the $D0_3$ matrix. Shown in Figure 7(b) is an SADP of the as-quenched alloy. In this figure, it is seen that in addition to the reflection spots with streaks of the L-J phase, the superlattice reflection spots with satellites lying along <001> reciprocal lattice directions could be clearly observed. Compared with the previous studies in the $Cu_{3-x}Mn_xAl$ alloys with x=0.5 or x=0.8 [1, 25], it is obvious that these supperlattice reflection spots with satellites were attributed to the coexistence of the ($D0_3$+$L2_1$) phases. The ($D0_3$+$L2_1$) phases could be formed via the $\beta \rightarrow B2 \rightarrow$ $D0_3$+$L2_1$ transition during quenching. Figure 7(c), a (002) $D0_3$ DF electron micrograph; no evidence of the a/4 <111> APBs could be detected. This feature is similar to that observed in the as-quenched $Cu_{3-x}Mn_xAl$ alloys with $0.5 \leqq x$

$\leqq$ 1.0 [1-2, 25]. Figures 7(d), a ($\bar{1}11$) $D0_3$ electron micrographs, reveals the presence of the $D0_3$ domains with a/2 <100> APBs. Figure 7(e), a DF electron micrograph taken with the ($0\bar{2}0$) L-J reflection spot, exhibits that the amount of the extremely fine L-J precipitates was greater than that observed in Figures 5 and 6. As a consequence, the as-quenched microstructure of the $Cu_{2.6}Mn_{0.4}Al$ alloy was the mixture of ($D0_3$+$L2_1$ +L-J) phases.

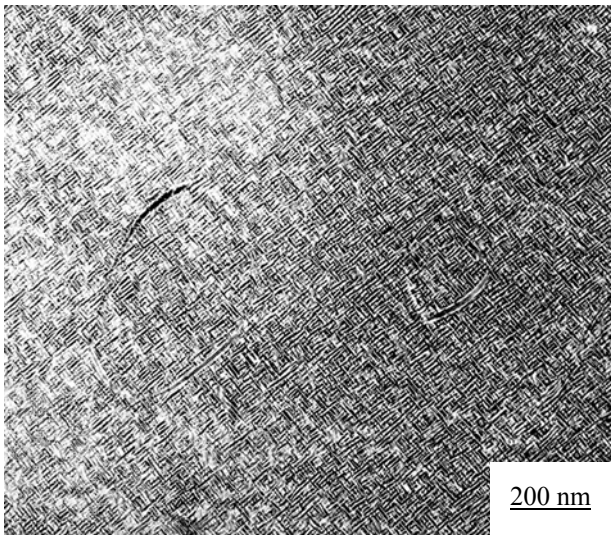

Fig. 7(a)

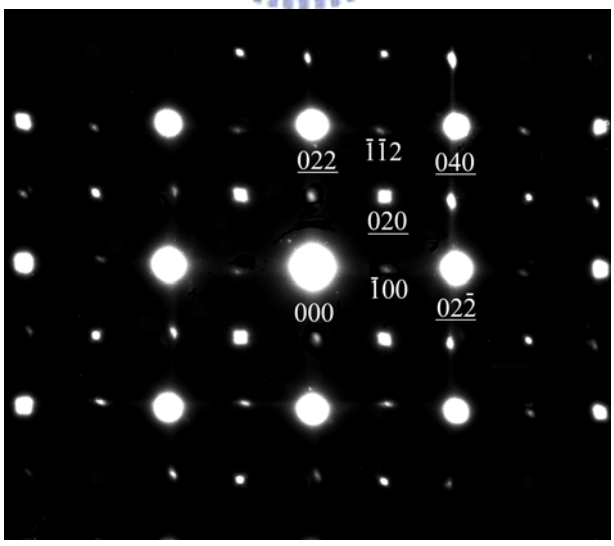

Fig. 7(b)

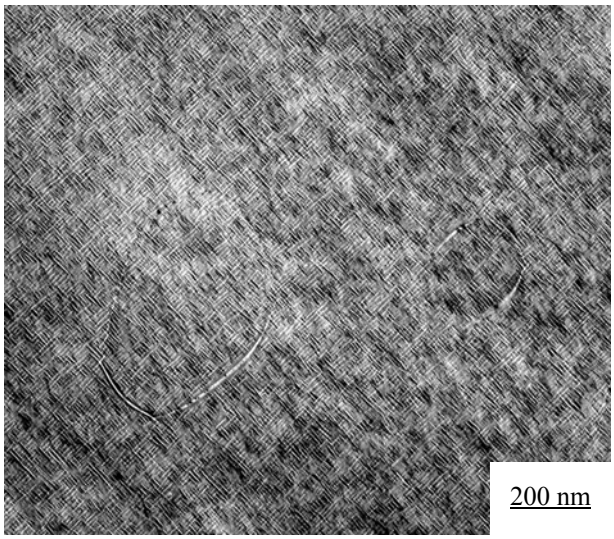

Fig. 7(c)

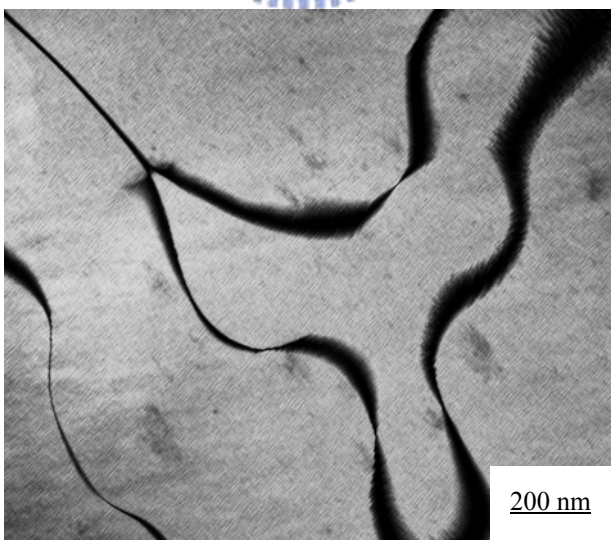

Fig. 7(d)

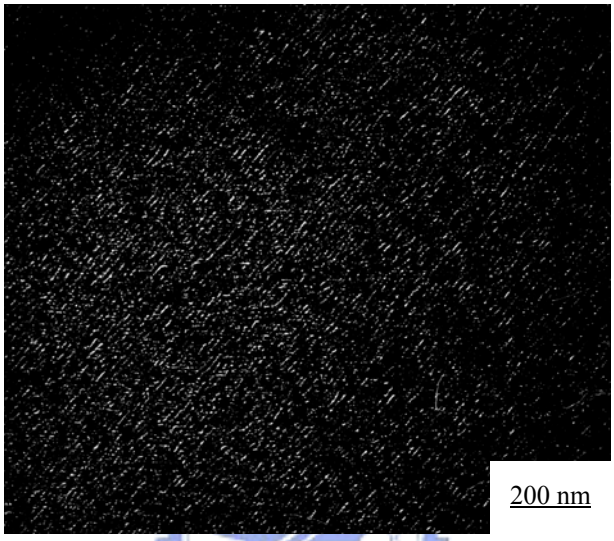

Fig. 7(e)

Fig. 7 Electron micrographs of the as-quenched alloy D. (a) BF, (b) SADP. The zone axes of the matrix are [001], (<u>hkl</u>= $D0_3$ + $L2_1$ phase, hkl= L-J phase,) (c) and (d) (002) and ($\bar{1}11$) $D0_3$ DF, respectively, (e) ($0\bar{2}0$) L-J DF.